2021

Effect of Subcooling Control on Residential Heat Pump Systems' Performance

Bruno Yuji Kimura de Carvalho
ACRC, the University of Illinois, Urbana, Illinois, USA, brunoykc@illinois.edu

Pega Hrnjak
ACRC, the University of Illinois, Urbana, Illinois, USA

Effect of Subcooling Control on Residential Heat Pump Systems' Performance

Bruno Yuji Kimura DE CARVALHO[1]*, Pega HRNJAK[1,2]*

[1]ACRC, University of Illinois at Urbana-Champaign,
Urbana, Illinois, USA
brunoykc@illinois.edu

[2]Creative Thermal Solutions Inc.
Urbana, Illinois, USA
pega@illinois.edu

* Corresponding Author

ABSTRACT

An electronic expansion valve can be used to improve efficiency and capacity in residential heat pump system by changing the focus of its control method on condenser subcooling and allowing slightly wet compressor suction to reduce discharge temperatures. This paper will present results of an experimental and theoretical analysis of the use of subcooling control. An investigation based on ideal cycle analysis shows potential improvements in HPF can be obtained if the subcooling is controlled by the system's expansion valve, but higher specific heating capacity and pressure ratios may reduce the overall improvement as outdoor temperatures are further decreased. A 2-Ton (7 kW) off-the-shelf residential system was used to evaluate the effect of subcooling control the system's performance characteristics under a range of external conditions for HSPF calculation and compared with the original system's expansion control. HPF (Heating performance factor) was increased by up to 19.1% in low load conditions and up to 4.2% in high load conditions. Heating capacity was also improved by up to 18.1%, which penalizes low load conditions by requiring more often on/off cycling but could lead to even higher HPF increase if the compressor speed is lowered to match the load of the residence in higher load conditions and can also improve efficiency at conditions that require auxiliary heating. HSPF was calculated for both subcooling controlled and baseline system showing an improvement of 19.2% in HSPF with a negative effect only observed between 0C and 5.5C which suffer from higher cycling degradation. The control scheme was defined as a linear function of the refrigerant condensation and indoor air inlet temperature difference. The control curve showed good agreement with both experimental and model data for the system, with the charge compensator causing some deviation from the rest of the data. The use of an accumulator as a charge receiver may eliminate the requirement of a charge compensator simplifying the cycle architecture while still providing an increase in efficiency with subcooling control.

1. INTRODUCTION

Cost reduction of electronic expansion valves (EXV) have enabled the widespread use of these components in residential air conditioning and heat pump systems. Despite the ability to fully control the expansion device to possibly maximize efficiency or capacity, most implementations still rely solely on superheat control. While controlling superheat can deliver acceptable performance and prevent any liquid intake at the compressor suction, it also presents some issues with minimum stable superheat which may lead to hunting (Chen et al., 2002). Performance improvement ranging from 2.7%-8.4% for mobile air conditioning systems have been obtained by Pottker and Hrnjak (2012 and 2015). The authors also showed that the potential for increase in coefficient of performance is inversely proportional to the size of the condenser. Xu and Hrnjak (2014) also obtained COP improvement in a residential air conditioning system with subcooling control when compared to the use of a conventional thermostatic expansion valve (TXV). Experimental results corroborating the benefit from COP-maximizinng subcooling and no evaporator superheat combined were presented by de Carvalho and Hrnjak (2019a).

Heating performance factor (HPF) improvement by means of subcooling stems from the overall greater relative increase in specific heating capacity as opposed to the specific compression work as the condensation pressure rises with higher subcooling. Figure 1a and equations (1) and 2 illustrate the change as subcooling is increased in a T-h

diagram, as the high-side pressure increases the enthalpy change on the condenser will be improved by the lower expansion device inlet enthalpy and higher discharge enthalpy, while only the increase in discharge enthalpy will boost specific compression work. By controlling subcooling the system can operate with no superheat on the evaporator, as shown in figure 1b, which not only reduces dryout, but can also mitigate maldistribution, increasing the HTC and consequently the evaporation pressure. A higher effectiveness in the evaporator will lead to a reduction in compressor power, due to lower pressure difference and higher mass flow rate boosting capacity. For heat pump application capacity improvements can reduce the need for auxiliary heating, especially at outdoor temperatures below -5°C, which will directly increase HPF. de Carvalho and Hrnjak (2019b) have previously shown that subcooling control in heat pump system can increase HPF and that this control strategy sacrifices some accuracy for a reduction in charge-sensitivity when compared to discharge superheat control.

$$\Delta q_{cond} = \Delta q + \Delta w \tag{1}$$

$$HPF' = \frac{q_c + \Delta q_e + \Delta w}{w + \Delta w} \tag{2}$$

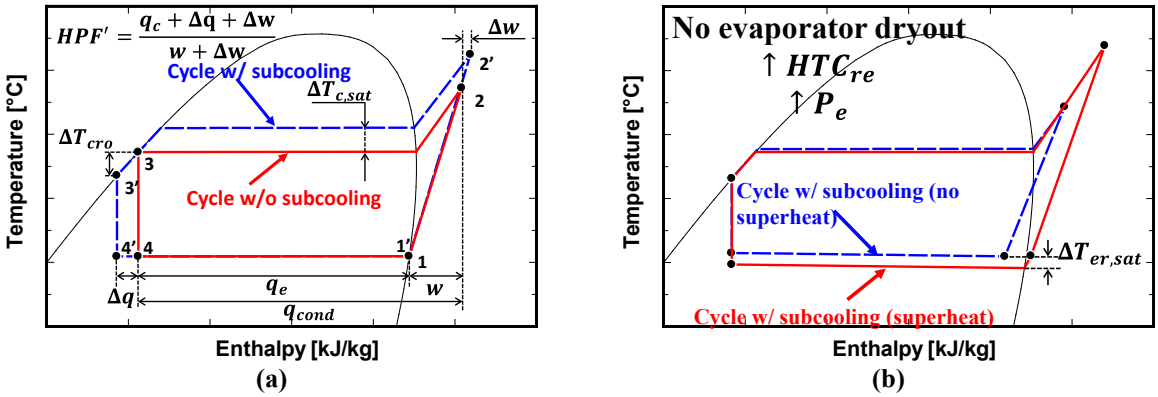

Figure 1: Maximum HPF as a balance of w and q increase with subcooling (a) and increased evaporator effectiveness when operating with no superheat and controlling expansion device through subcooling

Subcooling control in a heat pump water heater was able to significantly improve HPF when compared to a zero subcooling system (Pitarch et al., 2017). The authors also determined the higher performance was a consequence of higher exergy efficiency on the condenser and expansion device due to overall lower temperature difference between refrigerant and water in the condenser and decreased enthalpy at the expansion valve inlet.

Subcooling control may also be done indirectly through different variables, such as keeping a constant condenser approach (Hervas-Blasco et al., 2018) or even controlling discharge superheat (Tanawittayakorn et al., 2012; Menken et al., 2014).

In this paper the performance characteristics of a residential heat pump with subcooling control were assessed, and possible alternative subcooling control strategies were investigated. Results at the system's optimal points were compared to the data with the original baseline control.

2. THEORETICAL ANALYSIS

2.1 Ideal cycle analysis of potential benefits from subcooling control in heat pump

To evaluate the potential for HPF improvement in a heat pump cycle a similar analysis as the one performed by Pottker and Hrnjak (2012) was implemented based on the cycle represented in figure 1. Equation (3) shows an approximation for the increase in specific heating capacity for an ideal cycle assuming constant evaporation pressure and an increase in subcooling, as well as condensation pressure. Equation (4) shows the original specific heating capacity and finally eq. (5) is the relative increase in specific heating capacity based on the higher subcooling.

$$\Delta q_c \cong \overbrace{h_{2'} - h_2}^{\Delta w} + \overbrace{\overline{cp}_{l.c}(\Delta T_{cro})}^{\cong \Delta q_e} \tag{3}$$

$$q_c = h_2 - h_{c,sat,v} + h_{fg.c} \tag{4}$$

$$\frac{\Delta q_c}{q_c} = \frac{h_{2\prime} - h_2 + \overline{cp}_{l.c}(\Delta T_{cro})}{h_2 - h_{c,sat,v} + h_{fg.c}} \tag{5}$$

Considering an increase in subcooling of 5 K, and an increase in condensation temperature of 1 K table 2 shows the resulting relative increase in specific compression work, heating and cooling capacities. An initial condensation temperature of 45°C and evaporation temperature of 5°C were used in this analysis. The relative improvement in specific heating capacity is about 10% lower than the increase obtained for the cooling capacity. This decreased benefit in performance is mostly due to the overall larger initial heating capacity. Generally, a lower liquid specific heat and enthalpy of condensation leads to greater improvement from subcooling. The fluid used in this study's experimental analysis is R410a, which shows the highest relative increase in specific heating capacity among the refrigerants included in this analysis.

Table 1: Ideal cycle analysis of performance improvement from subcooling for a heat pump

Refrigerant	$Cp_{l.c}$ (kJ kg^{-1}K^{-1})	hfg_e (kJ kg^{-1})	hfg_c (kJ kg^{-1})	$\frac{\Delta w}{w}$ (%)	$\frac{\Delta q_c}{q_c}$ (%)	$\frac{\Delta q_e}{q_e}$ (%)	$\frac{\Delta HPF}{HPF}$ (%)
R410a	2.002	215.1	148.4	2.256	6.055	6.696	3.715
R134a	1.516	194.7	157.6	2.155	4.996	5.499	2.781
R1234yf	1.431	160.7	128.6	2.079	6.043	6.681	3.882
R290	2.97	367.5	295.8	2.168	5.202	5.749	2.97
R717	4.967	1244	1075	2.463	2.376	2.357	-0.08528
R600a	2.575	350.1	305.1	2.149	4.668	5.104	2.465
R32	2.221	1.814	223.99	2.374	4.445	4.812	2.023

The analysis was also done for lower evaporation temperatures to evaluate how much improvement could be obtained as the heat pump load in increased due to lower outdoor ambient temperatures. Fig. 2a and 2b show the change in relative change of the heating capacity and specific compression work as the saturation temperatures are varied, respectively. For a fixed condensation temperature, the decrease in Δqcond/qcond as the evaporation temperature drops is not as significant as the decrease in Δw/w which should lead to potentially higher performance improvement as the outdoor air ambient temperature is decreased. Since this analysis is based on an ideal cycle the isentropic efficiency of the compressor is not considered, but the effect obtained at lower evaporation temperatures should mitigate the decrease in compressor efficiency due to higher compression ratios and possibly lead to good performance improvement even at low outdoor ambient temperatures.

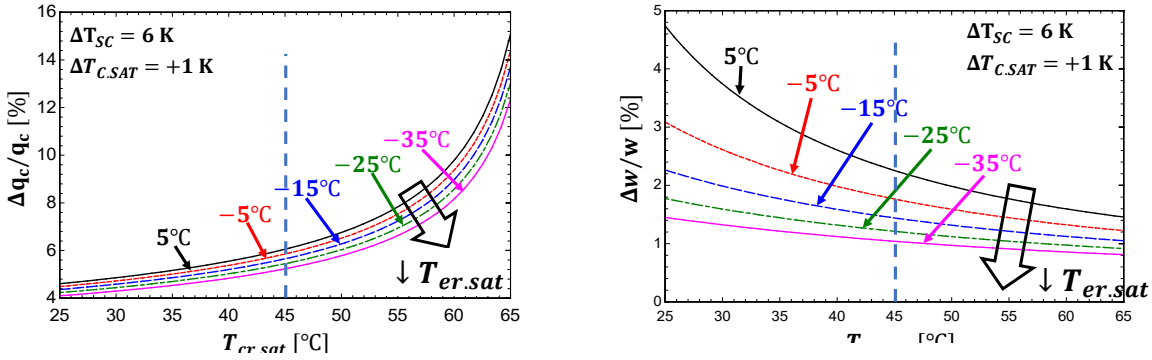

(a) (b)

Figure 2: Relative change in specific heating capacity and compression work as a function of condensation and evaporation temperatures

3. FACILITY

Figure 3 shows the full schematic for the facility used in this study. Two environmental chambers simulate indoor and outdoor conditions and can keep temperatures within ± 0.5°C and absolute humidity ±2%. Compressor, heaters and blowers power measurement is within ±0.2% and the expanded uncertainty for air-side and refrigerant side capacity calculations of approximately ±4%. Heating performance expanded uncertainty is estimated to be around ±5%.

4WV: 4-way valve
ABL: Air blender
ACC: Accumulator
AIR: Air
BL: Blower
CC: Charge compensator
CD: Condenser
CP: Compressor
DP: Differential pressure transducer
DPS: Dew-point sensor
EGC: Ethylene glycol chiller
EGHX: Ethylene glycol heat exchanger
ERH: Electric resistance heater
EV: Evaporator
EXV: Electronic expansion valve
FN: Flow nozzle
MF: Muffler
MFM: Mass flow meter
P: Absolute pressure transducer
SI: Steam injection
T: Type-T thermocouple
TCG: Thermocouple grid
TXV: Thermostatic expansion valve
VFD: Variable frequency drive

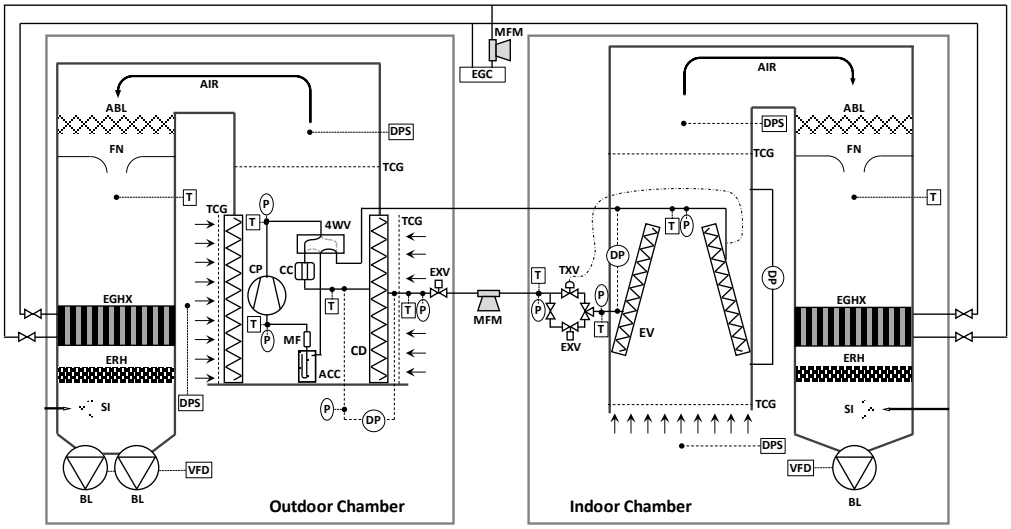

Figure 3: Layout of facility for performance evaluation

An off-the-shelf reversible residential 2 Ton (7kW) R410-A system with a round-tube A-coil indoor heat exchanger and a round-tube horizontal condenser with an electronic expansion valve (EXV) was installed in the facility. A separate EXV was installed on the outdoor unit to allow full control over the expansion process and the charge compensator was closed off from the system to prevent it from destabilizing subcooling control. The cycle diagram is shown in figure 4, the TXV on the indoor unit acts as a check valve during heat pump operation. Specifications for the indoor and outdoor heat exchangers are shown in Table 2.

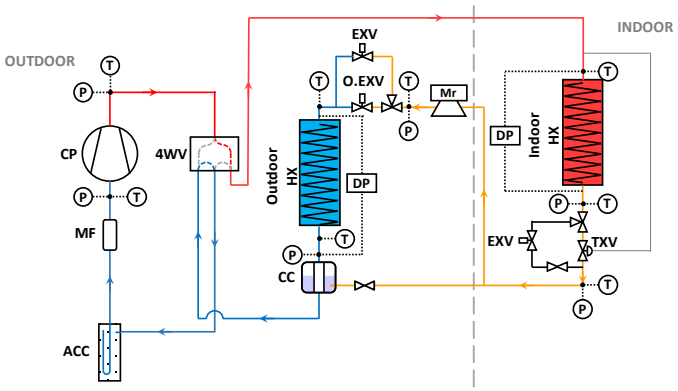

Figure 4: Schematic drawing of the air-conditioning system evaluated

Table 2: Residential system heat exchanger specifications

	Outdoor heat exchanger	Indoor heat exchanger
Description	2 rows, 8 circuits, 20 fpi	2 slabs, 3 staggered rows, 8 circuits, 14.5 fpi
Face area	2.81 m^2 (30.25 sqft)	0.689 m^2 (7.42 sqft)
Core depth	0.038 m	0.056 m
Core volume	0.1068 m^3	0.03858 m^3
Air side area	153.53 m^3	40.1 m^3
Refrigerant side area	4.61 m^3	2.39 m^3
Material	Aluminum fins, copper tubes, vapor line O.D. = 22 mm, liquid line O.D. = 9.5 mm	

4. EXPERIMENTAL RESULTS

4.1 Test conditions

To evaluate the HSPF improvement obtained by subcooling control the AHRI 210/240 heating conditions were used. The testing will follow the load increase as the outdoor temperature decreases with the system's maximum and minimum compressor speed defined by the control board. The test conditions are shown in table 3. 3 main conditions were tested. The indoor air flow rate also changes depending on a Full (maximum compressor speed) or Low (minimum compressor speed) conditions, from 900 down to 500 CFM, respectively.

Table 3: Heating performance testing conditions based on AHRI 210/240

Condition name	$H0_{Low}$	$H1_{Full}$	$H1_{Low}$	$H3_{Full}$
Outdoor DB temperature [°C]	16.7	8.33	8.33	-8.33
Outdoor WB temperature [°C]	13.6	6.11	6.11	-9.44
Outdoor AFR [CFM (m^3 s^{-1})]	2300 (1.085)	2300 (1.085)	2300 (1.085)	2300 (1.085)
Indoor DB temperature [°C]	21.1	21.1	21.1	21.1
Indoor WB temperature [°C]	15.6	15.6	15.6	15.6
Indoor AFR [CFM (m^3 s^{-1})]	500 (0.236)	900 (0.425)	500 (0.236)	900 (0.425)
Compressor speed [Hz]	30	53.33	30	95

The baseline system with its proprietary EXV control uses a nominal charge of 6600g. The charge selected for subcooling control of 8500g was based on the AFull condition for A/C operation assuming this condition would require the larger amount of charge to operate at its COP-maximizing subcooling. Heat pump operation generally need less refrigerant charge to properly operate because the internal volume of the condenser (indoor heat exchanger) is smaller. This system uses a charge compensator which should offset the charge imbalance between A/C and H/P operation by approximately 800 g. Testing showed that 6700 g would be enough for the H/P operation with subcooling control without a charge compensator, so the accumulator should hold around 1000g while controlling subcooling.

4.2 Subcooling control effect on system performance

Due to the different compressor speeds for each condition a separate analysis of the subcooling control effect will be shown in this section.

Figure 5 shows the T-h diagram for condition $H0_{Low}$, which is a partial load, low capacity condition. In this specific condition the baseline control defaults to a evaporator superheat control similar to the operation of a thermostatic valve. Due to the lower nominal charge the subcooling when running at 30 Hz for this partial load condition is of 1.5 K, with an HPF of 6.4. When subcooling control is used the system can be adjusted to operate at its HPF-maximizing value, found to be 5.5 K, higher than the baseline in part due to the low air flow rate set for the indoor heat exchanger.

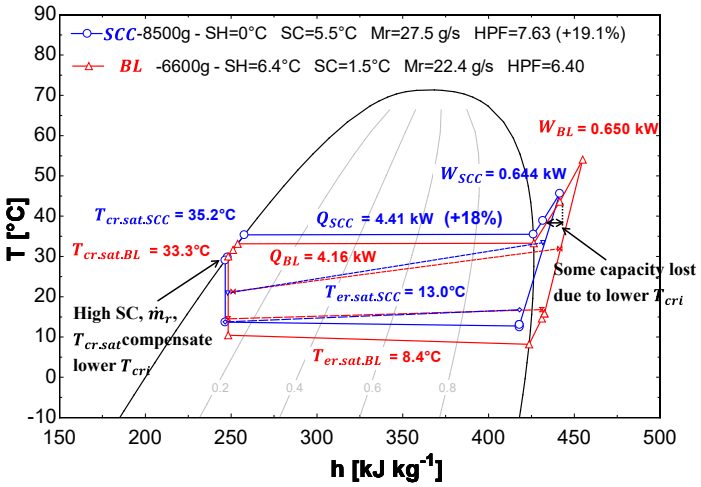

Figure 5: T-h diagram comparing the baseline system with a subcooling control-based system for $H0_{Low}$

Subcooling control in this case allow the evaporator to be flooded, with no dryout, thus increasing heat transfer coefficient, leading to an evaporation temperature 4.6 K higher than the baseline. Higher subcooling and elevated low side pressure also results in overall increased condensation temperature, 1.9K greater than the baseline. Subcooling control thus decreases pressure ratio and shows higher mass flow rates, caused in part by the higher suction density. Capacity is significantly increased by 18% while keeping the compressor work almost constant, this in turn improves HPF by 19.1%. The only downside of this improvement is that partial load conditions generally require cycling and operation with higher capacity would lead to increased cycling degradation losses. The HPF increase nonetheless should lead to higher HSPF values even after accounting for further cycling penalties.

The second condition analyzed was $H1_{Full}$, also considered the rating condition for heat pump systems. In general this condition has a higher weight on the HSPF and is better optimized by manufacturers. Figure 6 shows the T-h diagram comparison for this condition in which a smaller improvement in HPF of only 4.2% was obtained over the baseline control. The overall low subcooling of the baseline control indicates that the system may be undercharged for the heat pump operation even when using the nominal value optimized for the A/C operation. By operating with increased subcooling the improvements reflect figure 1 with lower condenser outlet enthalpy and no dryout in the evaporator which results in an increase in heating capacity and compressor power providing a balance that defines the maximum HPF obtained.

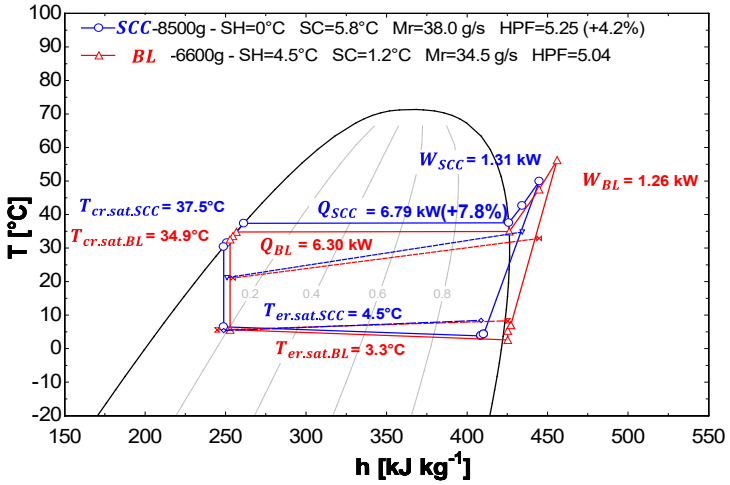

Figure 6: T-h diagram comparing the baseline system with a subcooling control-based system for $H1_{Full}$

The low load condition of $H1_{Low}$ shows a different operation for the baseline control. The system defaults to no superheat on the evaporator, but with close to zero subcooling, which in this case shows how much improvement can be obtained by simply operating at the correct HPF-maximizing subcooling.

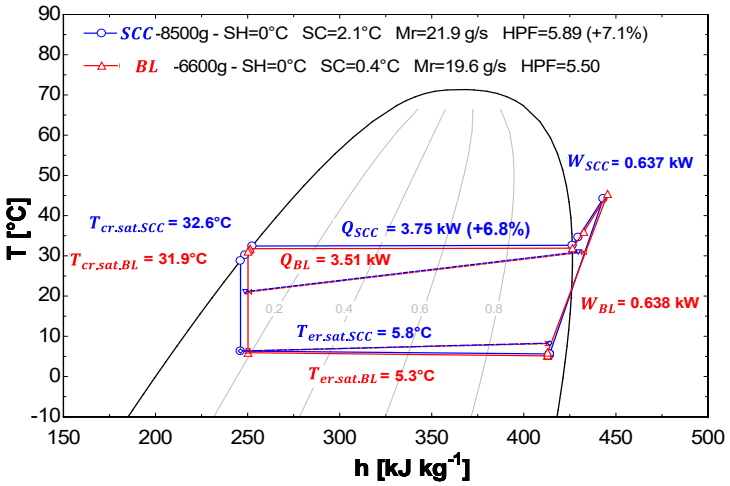

Figure 7: T-h diagram comparing the baseline system with a subcooling control-based system for $H1_{Low}$

Subcooling control achieves a 7.1% increase in HPF at an optimal subcooling of 2.1 K. The increase in efficiency is mostly originates from the higher capacity with lower condenser outlet enthalpy. Once again, this also indicates the charge compensator may be removing more active refrigerant charge than necessary in heat pump operation.

The lowest temperature condition $H3_{Full}$ show only a minor increase in HPF of 1.9% over the baseline, per figure 8. This small increase in efficiency is offset by the 18.1% capacity improvement which is beneficial for low temperature operation in heat pumps as it reduces the requirement of auxiliary heating to meet the load, leading to increase in overall system efficiency. In this case both baseline and subcooling control operate with no dryout on the evaporator and subcooling control has lower evaporation temperatures and operates with 11.1 K of subcooling. Capacity is increased by both higher condensation temperatures and lower condenser outlet enthalpy. If a thermostatic valve or evaporator superheat were used as the baseline another important advantage is that subcooling control can prevent high discharge temperatures due to not requiring superheat compressor suction.

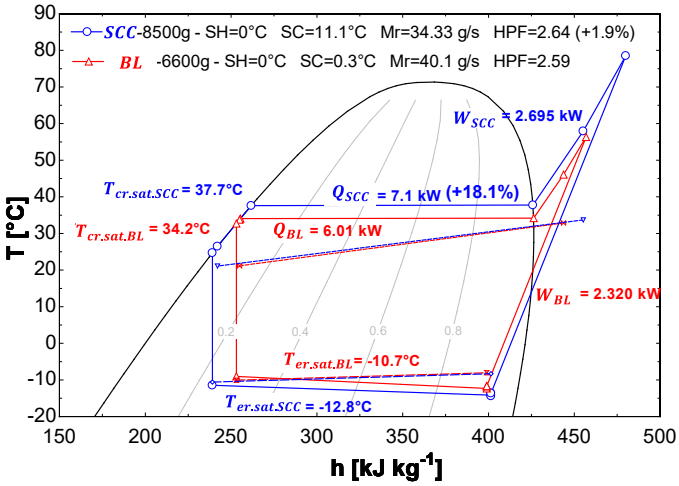

Figure 8: T-h diagram comparing the baseline system with a subcooling control-based system for $H3_{Full}$

4.3 HSPF improvement from subcooling control

Calculating HSPF requires interpolation of capacities and system power for all binned data using different weight based on seasonal occurrence of outdoor conditions. In this case Region IV was selected as it provided an intermediate case for heat pump operation. The design heating requirement selected for this analysis was the capacity at condition $H1_{Full}$ rounded up to 25000 Btu (7.33 kW). Table 4 shows the results for the HSPF calculations. Heat pump showed an improvement of 19.2%, almost twice as much as obtained in air conditioning by de Carvalho and Hrnjak (2021). The only area where some efficiency was lost was between 0 and 5.5°C, which showed lower efficiencies due to

higher cycling losses. Also the default heating degradation coefficient of 0.25 was used as the frost accumulation test was not performed.

Table 4: HSPF results for subcooling control and baseline

Condition name	Subcooling control	Baseline
HSPF [-]	14.3 (+19.2%)	12.0

4.4 Subcooling control scheme for heat pumps

By using the experimental data in this study along with data without a charge compensator and model data based on the system evaluated, a comprehensive linear control scheme was defined based on the temperature difference between refrigerant condensation and air inlet temperature, as shown in equation (6). This control strategy follows the approach defined by de Carvalho and Hrnjak (2019ab). In order to control subcooling three temperature sensor are required for heat pump operation: the indoor air temperature, condenser outlet temperature, and condenser saturation temperature, the latter of which is measured at the mid-point of one of the circuits of the indoor heat exchanger on the wall of the U-bend. Figure 9 shows that the presence of a charge compensator had some effect on the control curve when compared to the data without charge compensator. Since the accumulator will be used as the charge receiver for subcooling control a charge compensator may not be required simplifying the cycle architecture and providing a robust control scheme.

$$\Delta T_{SC} = 0.555\Delta T_{cra} - 1.4406 \quad (6)$$

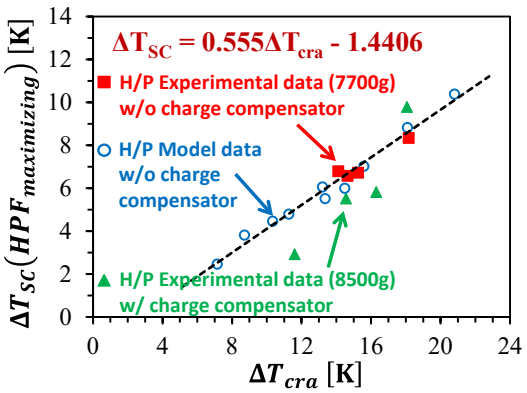

Figure 9: Heat pump subcooling control scheme based on experimental and model data

6. CONCLUSIONS

In this paper subcooling control was evaluated for a heat pump system and compared with the system's baseline control. Theoretical analysis of the effect of outdoor air temperature on subcooling control in heat pumps showed there is potential for HPF increase, but overall lower than COP in air conditioning due to the higher specific heating capacity relative to the specific compression work change.

HSPF improvement was determine by experimentally determining the HPF-maximizing subcooling for the required testing conditions and comparing with the baseline control. The original control employed by the system used evaporator superheat for high temperature conditions but defaulted to a different approach at low temperatures possibly to prevent excessively high discharge temperatures. With subcooling control it is possible to allow operation with no evaporator superheat under all conditions while still maximizing the HPF and using the accumulator to hold the excess charge of the system.

HPF was increased in all conditions, but improvement was lower at high load conditions, with 4.2% and 1.9% for, H1Full and H3Full, respectively, while significant increases were obtained for partial load conditions, with 19.1% and 7.1% increases for H0Low and H1Low, respectively. On the other hand, capacity was improved by up to 18.1% for all conditions, which can benefit low temperature conditions requiring less auxiliary heating, while it penalized partial load conditions which will demand more frequency on/off cycling. HSPF was overall increased by 19.2%, with penalties only between 0°C and 5.5°C which suffered from cycling degradation due to the increased capacities.

A linear curve for the control strategy was defined based on experimental and model data showing good agreement and simple implementation requirements.
This study has shown the potential for HSPF improvement by controlling subcooling and using the accumulator as a charge receiver. Further investigations must be performed on the reliability and stability of the control strategy, but the used of the control scheme presented in this paper could potentially lead to simple A/C and H/P expansion control capable of providing higher efficiency without increase in system architecture complexity.

NOMENCLATURE

AFR	Air volumetric flow rate	(m^3 s^{-1})
A/C	Air conditioning	
AFR	Air flow rate	(m^3 s-1)
BL	Baseline	
COP	Coefficient of performance	(–)
Cp	Specific heat capacity	(kJ $kg^{-1}K^{-1}$)
DB	Dry bulb	
EXV	Electronic expansion valve	
h	Enthalpy	(kJ kg-1)
H/P	Heat pump	
HPF	Heating performance factor	(-)
HSPF	Heating seasonal performance factor	
HTC	Heat transfer coefficient	(kW $kg^{-1}K^{-1}$)
m	Mass flow rate	(kg s-1)
P	Pressure	(kPa)
q	Specific cooling capacity	(kW kg^{-1})
Q	Capacity	(kW)
SC	Subcooling	(°C or K)
SCC	Subcooling control	
T	Temperature	(°C or K for differences)
TXV	Thermostatic expansion valve	
w	Specific work	(kW kg-1)
W	Work/Power	(kW)
WB	Wet bulb	

Subscript

a	air (subscript)
c	condenser (subscript)
e	evaporator (subscript)
fg	vaporization (subscript)
i	inlet (subscript)
l	liquid (subscript)
o	outlet (subscript)
r	refrigerant (subscript)
sat	saturation (subscript)
SC	subcooling (subscript)
v	vapor (subscript)

REFERENCES

de Carvalho, B.Y.K., Hrnjak, P. (2019). Performance Characteristics of a Residential Air Conditioning System with Subcooling Control. *Proceedings of the 25th International Congress of Refrigeration, Montreal, Canada* (1135). Paris, France: IIF/IIR

de Carvalho, B.Y.K., Hrnjak, P. (2019). Performance Evaluation and Strategies of Subcooling Control in Residential Heat Pump Systems. *Proceedings of the 25th International Congress of Refrigeration, Montreal, Canada* (1159). Paris, France: IIF/IIR

de Carvalho, B.Y.K., Hrnjak, P. (2021). Experimental and Theoretical Analysis of Subcooling Control in Residential Air Conditioning Systems. *Proceedings of the 18th International Refrigeration and Air Conditioning Conference at Purdue, West Lafayette, USA* (1159). West Lafayette, USA (2653). Purdue University.

Chen, W., Zhijiu, C., Ruiqi, Z., Yezheng, W., 2002. Experimental investigation of a minimum stable superheat control system of an evaporator. *Int. J. Refrigeration,* 25, 1137-1142.

Menken, J.K., Weustenfeld, T., Köhler, J., 2014. Experimental Comparison of the Refrigerant Reservoir Position in a Primary Loop Refrigerant Cycle with Optimal Operation. *Proceedings of the International Refrigeration and Air Conditioning Conference at Purdue, West Lafayette*, *USA.* West Lafayette, USA (1397). Purdue University.

Pitarch, M., Navarro-Peris, E., Gonzalvez-Macia, J., Corberan, J.M., 2017. Evaluation of optimal subcooling in subcritical heat pump systems. *Int. J. Refrigeration, 83, 18-31.*

Pottker, G., Hrnjak, P. S., 2012. Potentials for COP increase in Vapor Compression Systems, ACRC TR 294. University of Illinois at Urbana-Champaign.

Pottker, G., Hrnjak, P., 2015. Effect of the condenser subcooling on the performance of vapor compression system. *Int. J. Refrigeration, 50, 156-164.*

Tanawittayakorn, W., Phrajunpanich, P., Siwapornphaisam, S., 2012. Heat Pump Efficiency Improvement by Discharge Superheated Control. *Proceedings of the International Refrigeration and Air Conditioning Conference at Purdue, West Lafayette*, *USA.* West Lafayette, USA (1197). Purdue University.

Xu, L., Hrnjak, P.S., 2014. Potential of Controlling Subcooling in Residential Air Conditioning System ACRC TR311. University of Illinois at Urbana-Champaign.

Hervas-Blasco, E., Pitarch, M., Navarro-Peris, E., Corberán, J.M., 2018. Study of different subcooling control strategies in order to enhance the performance of a heat pump. *Int. J. Refrigeration, 88, 156-164.*

ACKNOWLEDGEMENT

This work was supported by the Air Conditioning and Refrigeration Center at the University of Illinois at Urbana-Champaign. Support from ACRC members and sponsors are gratefully acknowledged.